AD-A167 400 MEASUREMENT AND EXTRACTION OF RECURRING WAVEFORMS: FOR 1/1
APPLICATIONS TO AC..(U) NAVAL UNDERWATER SYSTEMS CENTER
NEW LONDON CT NEW LONDON LAB.. R F DWYER 24 MAR 86
UNCLASSIFIED NUSC-TM-861043 F/G 20/1 NL

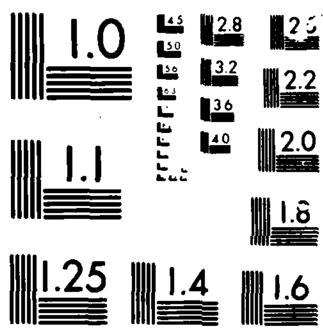

MICROCOP CHART

AD-A167 400

TM No. 861043

NAVAL UNDERWATER SYSTEMS CENTER
NEW LONDON LABORATORY
NEW LONDON, CONNECTICUT 06320

Technical Memorandum

MEASUREMENT AND EXTRACTION OF RECURRING WAVEFORMS:
FOR APPLICATIONS TO ACTIVE TRANSMISSIONS, FLOW-NOISE,
AND HELICOPTER-RADIATED NOISE PROBLEMS

DTIC ELECTE MAY 1 1986 S A D

Date: 24 March 1986

Prepared by: Roger F. Dwyer
Roger F. Dwyer
Surface Ship Sonar
Department

86 4 30 049

TM No. 861043

NAVAL UNDERWATER SYSTEMS CENTER
NEW LONDON LABORATORY
NEW LONDON, CONNECTICUT 06320

Technical Memorandum

MEASUREMENT AND EXTRACTION OF RECURRING WAVEFORMS: FOR APPLICATIONS TO ACTIVE TRANSMISSIONS, FLOW-NOISE, AND HELICOPTER-RADIATED NOISE PROBLEMS

Date: 24 March 1986

Prepared by: Roger F. Dwyer
Roger F. Dwyer
Surface Ship Sonar
Department

ABSTRACT

Physical acoustic sources that radiate transient waveforms represent a large class of noise generators. Active transmissions, flow-noise, and helicopter-radiated noise under certain flight situations depending on the source-observer orientation are members of this class. The objective of this paper is to present a signal processing methodology to extract time domain recurring waveforms from data. The recurring waveforms, on the one hand, may represent a source of interference that is to be eliminated as much as possible. But, on the other hand, these recurring waveforms may represent a desired signal that is to be extracted from a background of undesired noise. Both cases are shown in the paper to be different aspects of the same problem. Initially, the methodology is based on a physical property of equally spaced and identical recurring waveforms. These results are then generalized, because in practice, either by design or by other causes, the recurring waveforms may not be equally spaced and identical. The method is then applied to extract equally spaced and nearly identical waveforms which were produced by an approaching helicopter.

ADMINISTRATIVE INFORMATION

This technical memorandum was prepared under NUSC Project No. A75031, "Multidimensional Signal Processing," Principal Investigator Dr. Roger F. Dwyer (Code 3314), Program Manager Dr. N. Gerr, ONR (Code 411).

The author of this document is located at the
New London Laboratory, Naval Underwater Systems Center,
New London, Connecticut 06320.

INTRODUCTION

The data to be utilized, later in the paper, as an application to the signal processing methodology is from a helicopter. Therefore, a short discussion of aerodynamic noise generation appropriate for the application is presented initially. A more general discussion, then the one presented, can be obtained from the references cited. The discussion presented, however, will lead to the signal processing methodology which is the main topic of the paper. In addition, the signal processing methodology can be applied to active transmissions and flow-noise problems.

The theory of aerodynamic noise generation is based on Lighthill's [1] formulation of the wave equation

$$\frac{\partial^2}{\partial t^2} \rho(\underline{x},t) - c^2 \nabla^2 \rho (\underline{x},t) = \frac{\partial Q}{\partial t} - \frac{\partial F_i}{\partial X_i} + \frac{\partial^2 T_{ij}}{\partial X_i \partial X_j} \qquad (1)$$

where the right hand side is in tensor notation and represents sources of noise. The left hand side is the three-dimensional wave equation. In this equation the fluctuating density $\rho(\underline{x},t)$ measured at the observer's position $\underline{x}$ at time t, is related to the fluctuating pressure $p(\underline{x},t)$ by the equation $p=c^2\rho$, where c is the speed of propagation of sound.

These sources on the right of equation 1 are described in more detail by Lowson and applied to helicopter noise [2]. Lowson points out that the first term represents a simple source produced by mass introduction at a point which produces a monopole source. The second term represents sound produced by forces acting on the medium and can be described as a dipole source. Whereas, the last term is due to acoustic stresses and they radiate as a quadrupole source.

For a rigid surface in motion Ffowcs-Williams and Hawkins [3] obtained the exact solution of equation (1) as follows:

$$4\pi c^2 \rho(\underline{x},t) = \frac{\partial}{\partial t}\int \left[\frac{\rho_o u_n}{r\left|1-M_r\right|}\right] dS(\underline{Y}) - \frac{\partial}{\partial X_i}\int \left[\frac{p_{ij} n_j}{r\left|1-M_r\right|}\right] dS(\underline{Y}) + \frac{\partial^2}{\partial X_i \partial X_j}\int \left[\frac{T_{ij}}{r\left|1-M_r\right|}\right] dV(\underline{Y}) \tag{2}$$

where $p_{ij}n_j$ is the outward normal force per unit area exerted on the fluid by the surface of the body S, u_n is the outward normal component of the surface convection velocity $\underline{U}$, and ρ_o is the uniform density of the fluid at rest.

This equation was evaluated for rotors operating at supersonic tip speeds by Hawkings and Lowson [4]. In this case they assumed the blades were thin and therefore the last term of equation (2) could be neglected.

Since the acoustic radiated noise from the rotor is periodic they decomposed it into its harmonic components using Fourier analysis. Although more general, their results also agreed with results of Gutin [4].

The sources of aerodynamic radiated noise from a helicopter can be grouped into three categories [5, 6, 7]: 1) Rotational noise, or Gutin noise, which produces discrete frequencies at multiples of the blade passage frequency, 2) Broadband noise due to blade-turbulance interaction and 3) impulsive noise due to blade-vortex interactions and high tip speeds which also produce discrete frequencies, at multiples of the blade passage frequency, but at significantly higher levels than for Gutin noise.

In equation (2) the square brackets mean that the contents are to be evaluated at the retarded time, $\tau = t - r/c$, where $r = |\underline{X} - \underline{Y}|$ is the distance from the source $\underline{Y}$ to the observer. The other term, $1/|1 - M_r|$, is the doppler factor where M_r is the component Mach number in the direction of the observer.

An important physical insight to understanding the mechanism of helicopter impulsive noise was contributed by Schmitz and Yu [8]. They showed that the doppler factor gave a large pressure amplification as a

function of the azimuthal source position of the helicopter blade. Their description accounts for both the recurring impulses and directionality associated with helicopter-radiated impulsive noise. Essentially they showed that for an approaching helicopter impulses are heard in and near the plane of the main rotor and disappear entirely directly beneath the rotor. They attributed the mechanism of impulsive noise to sound arriving at the observer's position in-phase due to the sound emitted when the approaching blade's azimuthal position was almost perpendicular to the direction of the observer. For large component Mach numbers (approaching one) in the observer's direction impulsive noise would be heard and would recur at the blade passage frequency.

The time-domain theoretical results of reference [8] were compared with in-flight tests of an UH-1H helicopter [9] and with wind tunnel tests [10]. The theoretical results were found to be in good agreement with the real data except that the large negative pressure peaks associated with impulsive noise were always under predicted.

The objective of this paper is to present a signal processing method to extract recurring waveforms from a system so as to enhance a noisy measurement or to eliminate them as a source of interference.

Field measurements may be contaminated by other noise sources or the signal may be weak if measured at long ranges. In these cases it would be

advantageous to be able to enhance the time-domain data and improve interpretation and comparison with other data.

RECURRING TRANSIENTS

The physical principle of extracting recurring waveforms from data is contingent on obtaining discrete frequencies from its spectrum. Therefore, the methodology is based on frequency-domain processing [11]. This method relies on obtaining many equally spaced and identical waveforms over an interval of time. The spectrum of this data over the interval approaches a harmonically related line spectrum as the number of waveforms increase. The discrete frequencies contain all the useful information of the recurring waveforms over the interval. An enhancement occurs if the data of interest are composed of a relatively few line components distributed over a larger band. Therefore, this method enhances the time-domain data. In addition, in practice, this procedure will always be an approximation. Nevertheless, an example of a helicopter producing recurring waveforms presented later will show that the method is useful even for a short time interval of data. But, once the enhanced time domain data is available, subsequent frequency-domain processing may be applied.

Consider an acoustic waveform recurring every t' seconds. The pressure received at a sensor at time t can be expressed by the following equation [6],

$$p_r(t) = \sum_{n=-\infty}^{\infty} p(t-nt') ,$$

or in the frequency domain

$$p_r(\omega) = \omega_0 \, P(\omega) \sum_{n=-\infty}^{\infty} \delta(\omega - n\omega_0) \qquad (3)$$

where $\omega_0 = 2\pi/t'$, and $P(\omega)$ is the Fourier transform of the transient pressure $p(t)$.

Equation (3) implies that for a recurring waveform, $p(t)$, its associated frequencies are all discrete and are harmonically related to ω_0. For the case of helicopter-radiated noise ω_0 is the blade passage frequency [6]. But in practice we may not have an infinite number of recurring waveforms. However, for a stationary source [6, 7, 12] this can be approximated to a high degree. In the experiments of Schmitz and Boxwell [9] they were able to obtain a large number of recurring waveforms for a source in motion. In this case, the frequencies were doppler shifted.

For the data to be presented later the source was approaching a fixed observer and therefore the radiated waveforms were nonstationary over time with respect to the fixed observer. Therefore, only over a short interval of time could the data be assumed stationary.

In the rest of the paper the data are assumed to be filtered to the desired passband and appropriately A/D converted.

Let the received discrete data be given by the expression

$$x(i) = \sum_{k=0}^{w-1} A_k \, h[i-(i_g+kt')] \tag{4}$$

where $i=0,1,2,\ldots,N-1$ are the discrete temporal samples and w is the number of waveforms occurring over the interval of N uniformly spaced samples. For convenience the sampling interval is assumed to be equal to one. The other parameters are as follows:

- i_g - The sample on which the first waveform starts.
- t' - Temporal separation of waveforms, given as an integral number of samples.
- h - Basic shape of waveform.
- A_k - Amplitude of k-th waveform.

Since the waveforms are constrained to occur over a finite interval of N samples the following inequality must hold

$$o \leq kt' \leq N-1-i_g-\Delta$$

where Δ is the width of the waveform.

Transforming x(i) to the frequency domain we obtain the spectrum

$$X(K) = (1/\sqrt{N}) \sum_{i=0}^{N-1} x(i)\ ex(i) \tag{5}$$

where $K=0,1,2,\ldots,N-1$ and we have defined the expression $ex(\ ) = e^{-j2\pi K(\ )/N}$.

The spectrum of equation (4) is given by

$$X(K) = (1/\sqrt{N}) \sum_{k=0}^{W-1} W(K,k)\ ex(i_g+kt')$$

where

$$W(K,k) = \sum_{r=-(i_g+kt')}^{N-1-(i_g+kt')} A_k h(r)\ ex(r) \qquad (6)$$

However, for the class of functions, $h(r)$, being considered here

$$W(K,k) = A\ W(K).$$

For example, let

$$\begin{aligned} h(r) = \quad & -(1/4)\ \delta(r+t_2) - (1/2)\ \delta(r) - (1/4)\ \delta(r-t_2) \\ & + (1/2)\ \delta(r+t_2-t_1) + \delta(r-t_1) + (1/2)\ \delta(r-t_2-t_1) \\ & - (1/4)\ \delta(r+t_2-2t_1) - (1/2)\ \delta(r-2t_1) - (1/4)\ \delta(r-t_2-2t_1) \end{aligned}$$

where $\delta(\ )$ is the Kronecker delta function and the following inequalities hold:

$$o < t_2 < 2t_2 < t_1 < 2t_1 < \Delta \quad ,$$

$$o \leq \Delta + i_g + kt' \leq N-1 \quad , k=0,1,2,\ldots,w-1.$$

The function, h(r), is plotted in figure 1 for three recurring impulse functions. We also constrained h(r) to have an average value equal to zero over the interval. This will insure that its power spectrum is zero at K=0.

From equation (6) we obtain the expression,

$$W(K) = [1+\cos(2\pi Kt_2/N)]\ [1-\cos(2\pi Kt_1/N)]\ ex(t_1)$$

and the spectrum for this example is given by

$$X(K) = (Aw/\sqrt{N})\ [1+\cos(2\pi Kt_2/N)]\ [1-\cos(2\pi Kt_1 N)]\ ex(t_1)$$
$$\cdot\ ex(i_g + \frac{w-1}{2}\ t')\ \left[\frac{\sin(\pi wKt'/N)}{w\sin(\pi Kt'/N)}\right] \qquad (7)$$

The peaks of equation (7) can be conveniently found from its, unaveraged, magnitude squared or, power spectrum, which is given by

$$\left|X(K)\right|^2 = (A^2w^2/N)\ [1+\cos(2\pi Kt_2/N]^2\ [1-\cos(2\pi Kt_1/N)]^2$$
$$\cdot\left[\frac{\sin(\pi wKt'/N)}{w\ \sin(\pi Kt'/N)}\right]^2 \qquad (8)$$

where the expression $[1+\cos(2\pi Kt_2/N)]^2\ [1-\cos(2\pi Kt_1/N]^2$ controls the overall shape by the locations of its zeros. Whereas,

$$\frac{\sin(\pi\ wKt'/N)}{w\ \sin(\pi Kt'/N)} \tag{9}$$

give the locations of the peaks of the power spectrum from the solutions to the equation

$$\sin(\pi Kt'/N) = 0$$

which are given by

$$K = (N/t')\ I_o$$

for, $0 \leq K \leq N-1$ and $I_o = 0, \pm 1, \pm 2, \ldots$.

Therefore, t' controls both the number and locations of the discrete components. As $w \to \infty$, equation (9) will approach a unit delta function so that the spectrum becomes a purely line spectrum.

The power spectrum of equation (8) is plotted in figure 2 for set of realistic parameters which correspond with the helicopter data that will be presented later. The parameter set is as follows: N = 1024, w = 12, A = .3 Volts, T_2 = 1 msec, t_1 = 4 msec, and t' = 83 msec.

EXTRACTION

The previous example showed that a recurring process produced a power spectrum with sharp peaks. Therefore, most of the information was contained at these peaks. This phenomenon is the basis for the extraction method.

Rewriting equation (7) in the following way

$$X(K) = (AW/\sqrt{N})\ W(K)\ \mathrm{ex}(i_g + \frac{w-1}{2} t') \left[\frac{\sin(\pi wKt'/N)}{w\sin(\pi Kt'/N)}\right] \qquad (10)$$

reveals the extraction procedure. The term

$$\frac{\sin(\pi wKt'/N)}{w\sin(\pi Kt'/N)}$$

represents the locations of the peaks. These solutions form a solution space denoted by S. The discrete frequencies representing the solution space will be denoted by the expression $K \epsilon S$.

The extracted data are found by transforming X(K), for all $K \epsilon S$, into the time-domain by applying an inverse discrete Fourier transform (IDFT) as follows:

$$x_E(i) = (1/\sqrt{N}) \sum_{K \epsilon S} X(K)ex(-i)$$

and from equation (10),

$$x_E(i) = (Aw/N) \sum_{K \epsilon S} W(K)\ ex\left\{-[i-\ (i_g+\frac{w-1}{2}\ t')]\right\} \qquad (11)$$

In practice the inverse fast Fourier transform is utilized so that the method is highly efficient.

Now the resultant data, left after the extraction process, is obtained from the equation

$$x_R\ (i) = x(i) - x_E(i) \tag{12}$$

where,

$$x_R(i) = (Aw/N) \sum_{K \notin S} W(K) \quad ex \left\{ -[i-(i_g + \frac{w-1}{2}\ t')]\right\} \left[\frac{\sin(\pi Kt'\ /N)}{w\sin(\pi Kt'/N)}\right]$$

so that the original data is the sum of the extracted and resultant components,

$$x(i) = x_E(i) + X_R(i).$$

These ideas can be discussed in terms of matrices and vectors. This is called the matrix method.

Let

$$\underline{x} = (x(0),\ x(1),\ \ldots,\ x(N-1))^T$$

be a vector of time domain data samples. Here T represents transpose.

Similarly, the frequency domain data is given by the vector

$$\underline{X} = (X(0),\ X(1),\ \ldots,\ X(N-1))^T$$

where the two vectors are related through the transformation

$$\underline{X} = F\ \underline{x}$$

and F is a (NxN) transform matrix representing the DFT operation as follows:

$$F = (1/N)^{1/2} \begin{bmatrix} 1 & 1 & 1 & \cdots & 1 \\ 1 & \exp(-j2\pi/N) & \exp(-j2\pi 2/N) & \cdots & \exp(-j2\pi(N-1)/N) \\ 1 & \exp(-j2\pi 2/N) & \exp(-j2\pi 4/N) & \cdots & \exp(-j2\pi 2(N-1)/N) \\ . & & & & \\ . & & & & \\ . & & & & \\ 1 & \exp(-j2\pi(N-2)/N) & \exp(-j2\pi 2(N-2)/N & \cdots & \exp(-j2\pi(N-2)(N-1)/N) \\ 1 & \exp(-j2\pi(N-1)/N) & \exp(-j2\pi 2(N-1)/N) & \cdots & \exp(-j2\pi(N-1)(N-1)/N) \end{bmatrix}$$

and its inverse exists and is denoted by

$$F^{-1} = (1/N)^{1/2} \begin{bmatrix} 1 & 1 & 1 & \cdots & 1 \\ 1 & \exp(j2\pi/N) & \exp(j2\pi 2/N) & \cdots & \exp(j2\pi(N-1)/N) \\ 1 & \exp(j2\pi 2/N) & \exp(j2\pi 4/N) & \cdots & \exp(j2\pi 2(N-1)/N) \\ . & & & & \\ . & & & & \\ . & & & & \\ 1 & \exp(j2\pi(N-2)/N) & \exp(j2\pi 2(N-2)/N) & \cdots & \exp(j2\pi(N-2)(N-1)/N) \\ 1 & \exp(j2\pi(N-1)/N) & \exp(j2\pi 2(N-1)/N) & \cdots & \exp(j2\pi(N-1)(N-1)/N) \end{bmatrix}$$

We will now define a diagonal (NxN) operator matrix Q which is applied in the frequency domain.

The frequency domain resultant data is then represented in the form

$$\underline{X}_R = [F-QF]\,\underline{x}$$

Applying the inverse transformation we obtain

$$\underline{x}_R = \underline{x} - F^{-1}QF\,\underline{x}.$$

If Q=I (identify matrix), then, $\underline{x}_R = \underline{0}$ (zero vector).

Whereas, if Q = 0 (zero matrix), then, $\underline{x}_R = \underline{x}$.

Therefore we can choose Q to obtain the desired result.

In addition,

$$\underline{x}_E = F^{-1}QF\,\underline{x}$$

is the extracted data vector

In applications the elements of diagonal matrix Q are chosen to represent the locations where the discrete components occur in the frequency domain i.e., $K \epsilon S$.

For example, let N=1024, and let there be four exact solutions located at K=0, 256, 512, and 768.

Then Q, = diag $[q_{ij};\ i,j=0,1,\ldots,1023]$

where,

$$q_{ij} = \begin{cases} 1, \text{ at } i=j = 0, 256, 512, \text{ and } 768 \\ 0, \text{ otherwise} \end{cases}$$

Therefore,

$$F^{-1}QF = (4/N)E$$

where,

$$E = \begin{bmatrix}
1\,0\,0\,0\,1\,0\,0\,0\,1\ldots0\,0\,0\,1\,0\,0\,0 \\
0\,1\,0\,0\,0\,1\,0\,0\,0\,1\ldots0\,0\,0\,1\,0\,0 \\
0\,0\,1\,0\,0\,0\,1\,0\,0\,0\,1\ldots0\,0\,0\,1\,0 \\
0\,0\,0\,1\,0\,0\,0\,1\,0\,0\,0\,1\ldots0\,0\,0\,1 \\
1\,0\,0\,0\,1\,0\,0\,0\,1\,0\,0\,0\,1\ldots0\,0\,0 \\
. \\
. \\
. \\
0 \\
0 \\
0 \\
1\,0\,0\,0\,1\,0\,0\,0\,1\ldots0\,0\,0\,1\,0\,0\,0 \\
0\,1\,0\,0\,0\,1\,0\,0\,0\,1\ldots0\,0\,0\,1\,0\,0 \\
0\,0\,1\,0\,0\,0\,1\,0\,0\,0\,1\ldots0\,0\,0\,1\,0 \\
0\,0\,0\,1\,0\,0\,0\,1\,0\,0\,0\,1\ldots0\,0\,0\,1
\end{bmatrix}$$

(1024 x 1024)

So the extracted data vector for this example is found from the expression

$$\underline{x}_E = (4/N)\ E\ \underline{x} = \underline{x}$$

The extracted data vector was equal to the original data vector because in this example all the information was located at discrete frequencies. Now if we add noise of the form $\underline{n}$ then

$$\underline{z} = \underline{x} + \underline{n}$$

and

$$\underline{z}_E = (4/N)\ E\ \underline{x} + (4/N)\ E\ \underline{n}$$

$$= \underline{x} + (4/N)\ E\ \underline{n} \qquad (13)$$

which reduces to, $\underline{z}_E \sim \underline{x}$. Since the noise is random, the noise vector will not match the transformation E and consequently the second term on the right side of equation (13) will be small.

The resultant data vector is obtained from the expression,

$$\underline{x}_R = \underline{x} - (4/N)\ E\ \underline{x} = 0.$$

Adding noise again we obtain

$$\underline{z}_R = \underline{n} - (4/N)\ E\ \underline{n} \sim \underline{n} \qquad (14)$$

Therefore, for this example, the extraction method is nearly perfect even with additive noise. In practice the matrix method will be limited by the ability to choose the appropriate operator matrix Q. In this regard we have shown the physical connection between the peaks in the spectrum (or solutions of equation (9)) and the operator matrix. But the matrix method is a purely mathematical procedure. Therefore, we can generalize this procedure to handle other situations that can occur in the time domain but do not have an obvious physical connection in the frequency domain.

Therefore, let E_g be a (NxN) matrix with elements

$$[g_{ij};\ i,\ j=0,1,2,\ldots,\ N-1].$$

Then,

$$\underline{x}_E = E_g\ \underline{x} \text{ and } \underline{x}_R = \underline{x} - E_g\ \underline{x}$$

are the extracted and resultant vectors for the generalized transformation matrix E_g.

In this generalized formulation $\underline{x}$ need not represent a vector of uniformly spaced and identical recurring waveforms. Rather, the recurring waveforms can have unequal separations with arbitrary amplitudes. In fact, the shapes need not be the same over the interval. However, the elements of the generalized transformation matrix must contain this knowledge in order to match the data vector. This information may be obtained, perhaps, from a learning procedure or, on the other hand, it may be known a priori as in a coded message.

In the next section we shall consider a segment of real data that contain recurring waveforms produced in a system by an approaching helicopter.

RESULTS

The details of the data acquisition were discussed in reference 11. Essentially, data from an approaching UH-1 helicopter were recorded from a microphone mounted 2 meters above the ground. A one second segment of far-field data were analyzed after being bandpassed filtered and sampled at 1024 samples per second using a 12 bit A/D converter. The band was from 50-400 Hz.

The, unaveraged, power spectrum estimate of this one second interval of data is shown in figure 3. A 1024-point FFT was used to obtain the frequency domain data. Therefore, the frequency resolution was 1 Hz. The power spectrum in figure 3 is characteristic of helicopter-radiated noise as discussed in reference 5. Here, however, only the main rotor frequency components are discernable in the figure. The peaks are indicated by arrows. Apparently, this was due to the range of the helicopter. Subsequent, closer-in, segments revealed contributions from both main and tail rotors.

These eight frequency components indicated in the figure by arrows will be utilized to obtain the extracted and resultant data components. Actually, however, the adjacent samples will be included. This gives a total of 48, out of the possible 1024 samples, incorporated in the extracted components.

During the approach of the helicopter impulsive noise could be clearly heard. These recurring waveforms are shown in the top graph of figure 4. Over the one second interval there are 12 recurring waveforms. Whereas, the time interval between waveforms is 82 msec. This corresponds to, approximately, a blade passage frequency of 12 Hz. The indicated frequencies of figure 3 are all multiples of 12 Hz. But due to the bandpass filter employed, the multiples below 50 Hz are not discernable and,

therefore, not included in the extraction procedure. This means that the fundamental frequency is not needed to reconstruct the proper time occurrences of the waveforms. The reason is that this information is already contained in the eight discernable frequency multiples. However, to reconstruct the individual waveform exactly all the frequencies associated with the pulse must be extracted.

The middle graph of figure 4 represents the resultant data after the eight indicated frequencies are extracted. Whereas, the extracted data are shown in the bottom graph. From these plots it is clear that the eight indicated frequencies represent the original waveforms to an extent. But the result are only an approximation. The time occurrences are maintained in the extracted data but the shape is distorted. Nevertheless, depending on the application, these results could be beneficial. For example, in a noisy environment the time domain data may be obscured. As long as the frequency components are still discernable the extracted data would give an enhancement. As was shown in the theoretical discussing, extending the interval and including more waveforms would increase the discernability of the frequency components.

The possible enhancement is demonstrated in figure 5. The original data with additive computer noise, at a -7 dB signal-to-noise level (measured in the time domain), is shown is the top graph. With this signal-to-noise level the eight frequency components were still

discernable. As in figure 4, the middle graph is the resultant data after the eight frequency components are extracted. The bottom graph representing the extracted data clearly shows the time domain enhancement.

The sensitivity of the extraction procedure to random Gaussian noise is demonstrated in figure 6. Here an analog Gaussian source was processed in a similar manner to the original helicopter data. As in the previous figures, the top graph is the original Gaussian noise data. The middle and bottom graphs are, respectively, the resultant and extracted data. These results also correspond with the theoretical predictions of sensitivity to random noise given by the matrix method.

SUMMARY AND CONCLUSIONS

In this paper a signal processing methodology was presented to extract recurring waveforms from data. The procedure was based on the principle that information associated with recurring waveforms is contained in discrete frequencies. Therefore, it was assumed, initially, that the recurring waveforms were uniformly spaced and identical. Under this assumption a physical connection between time and frequency domains was demonstrated. However, from the time domain development a purely mathematical generalization of the procedure was revealed based on a transformation matrix. This allowed a relaxation of the constraints originally required for the extraction procedure.

The signal processing procedure was demonstrated with helicopter-radiated noise data. It was shown that the extraction procedure could be useful to either remove recurring waveforms from data of interest or, on the other hand, to enhance a noisy time domain signal. These results are currently being generalized for an array of sensors.

ACKNOWLEDGMENT

This research was supported by the Office of Naval Research under research project RR014-05-OH.

REFERENCES

1. M. J. Lighthill, "On Sound Generated Aerodynamically: I. General Theory," Proc. Roy. Soc. A, 211, 564-587, 1952.

2. M. V. Lowson, "Basic Mechanisms of Noise Generation by Helicopters, V/STOL Aircraft and Ground Effect Machines," J. Sound Vib. Vol. 3, No. 3, 454-466, 1966.

3. J. E. Ffowcs Williams and D. L. Hawkings, "Sound Generated by Turbulence and Surfaces in Arbitrary Motion," Philosophical Transactions of the Royal Society, A264, 321-342, 1969.

4. D. L. Hawkings and M. V. Lowson, "Theory of Open Supersonic Rotor Noise," Journal of Sound and Vibration, 36(1), 1-20, 1974.

5. Lowson and Ollerhead, "A Theoretical Study of Helicopter Rotor Noise," J. Sound Vib., 9)2), 197-222, 1969.

6. S. Widnall, "Helicopter Noise Due to Blade-Vortex Interaction," J. Acoust. So. Amer. 50(1), 354-365, 1971.

7. Hubbard and Harris, "Model Helicopter Rotor Impulsive Noise," J. Sound Vib., 78(3), 425-437, 1981.

8. F. H. Schmitz and Yung H. Yu, "Theoretical Modeling of High-Speed Helicopter Noise," Journal of the American Helicopter Society, Vol. 24, 10-19, Jan. 1979.

9. F. H. Schmitz and D. A. Boxwell, "In-Flight Far Field Measurement of Helicopter Impulsive Noise," Journal of the American Helicopter Society, Oct. 1976.

10. F. W. Schmitz, D. A. Boxwell, and C. R. Vause, "High-Speed Helicopter Impulsive Noise," Journal of the American Helicopter Society, 28-36, Oct. 1977.

11. R. F. Dwyer, "Extraction of Helicopter-Radiated Noise by Frequency-Domain Processing," J. Acoust. So. Amer. 78(1), 95-99, July 1985.

12. D. B. Hanson, "Helicoidal Surface Theory for Harmonic Noise of Propellors in the Far Field," AIAA Journal, Vol. 18, No. 10, 1213-1220, 1980.

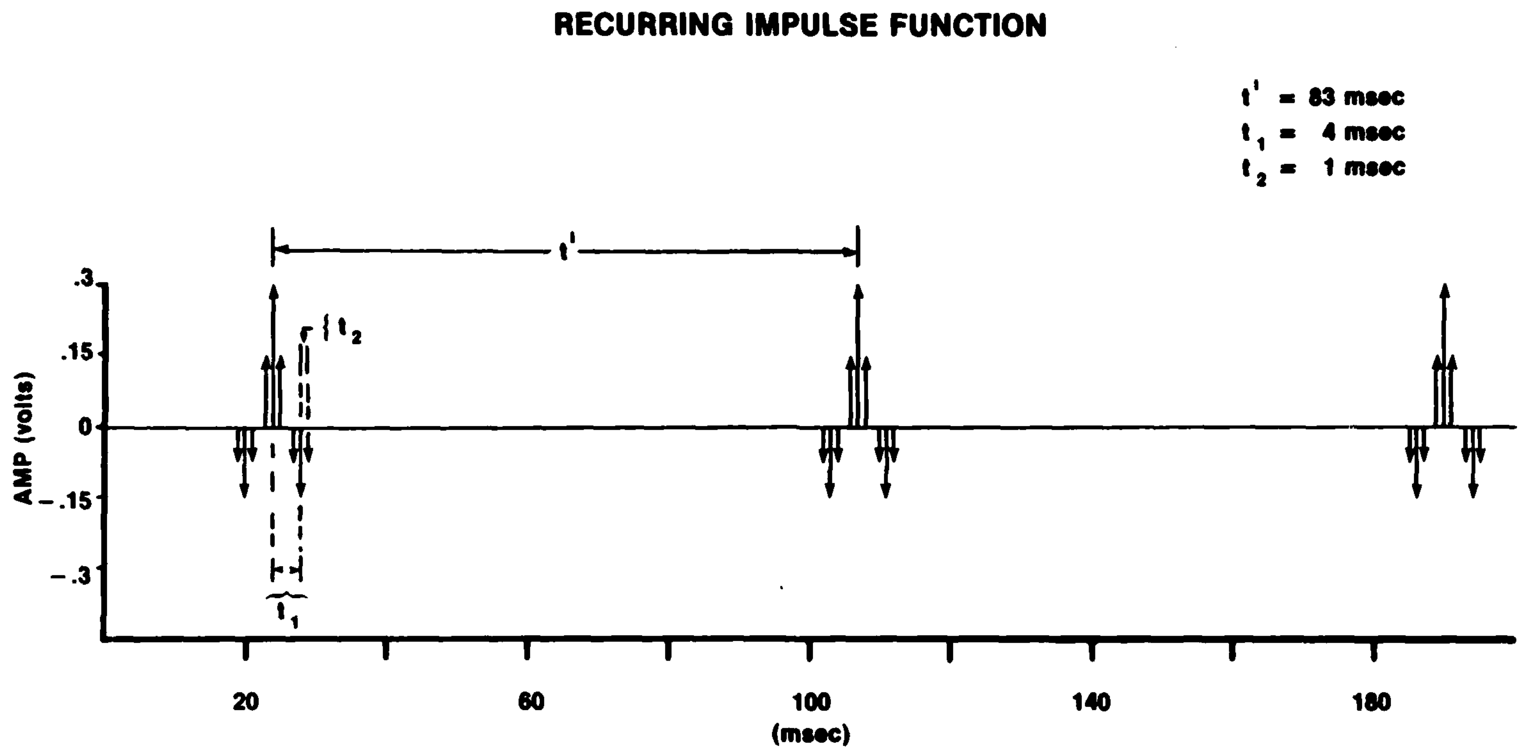

Figure 1. Recurring Impulse Function.

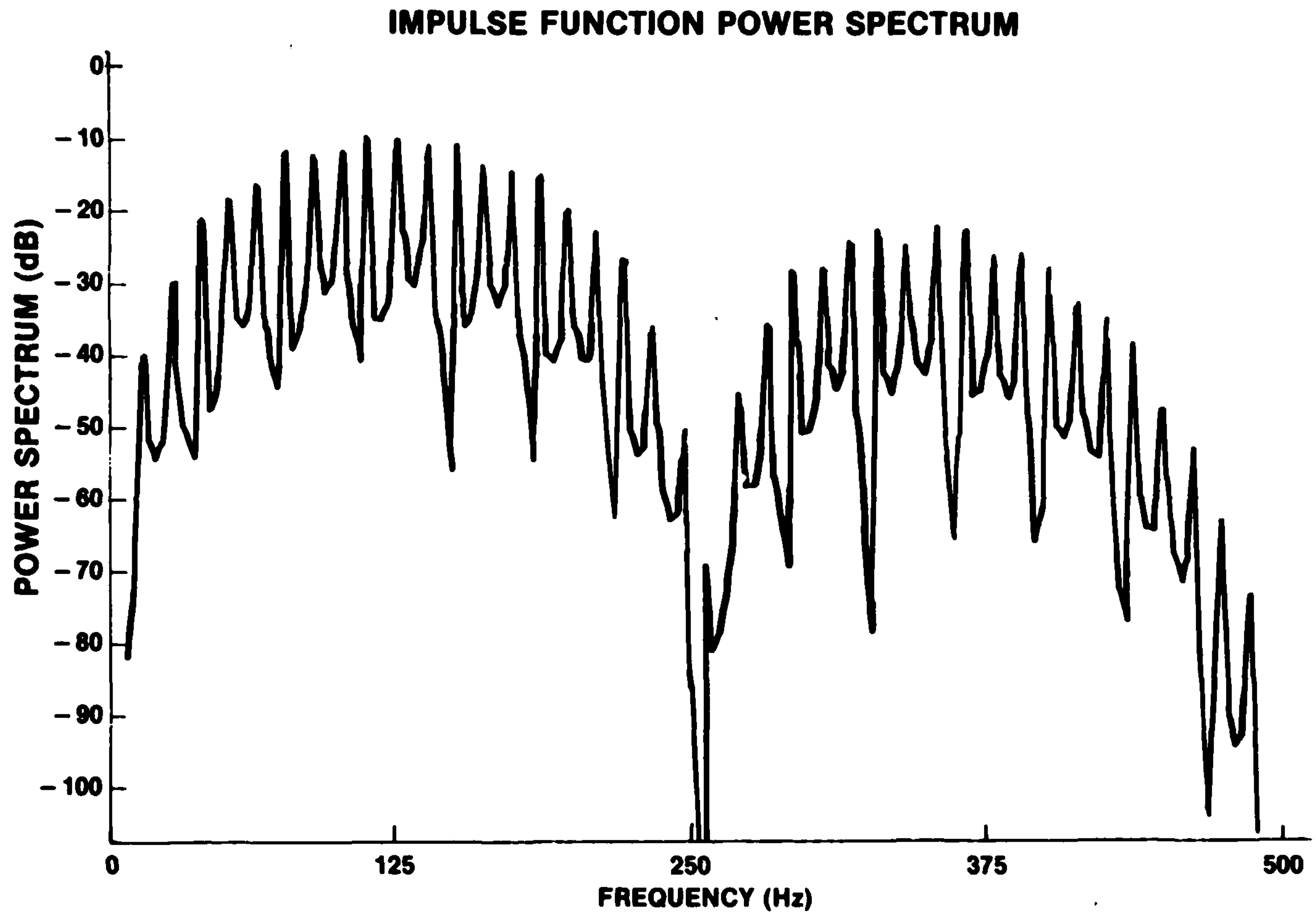

Figure 2. Power Spectrum of Recurring Impulse Function.

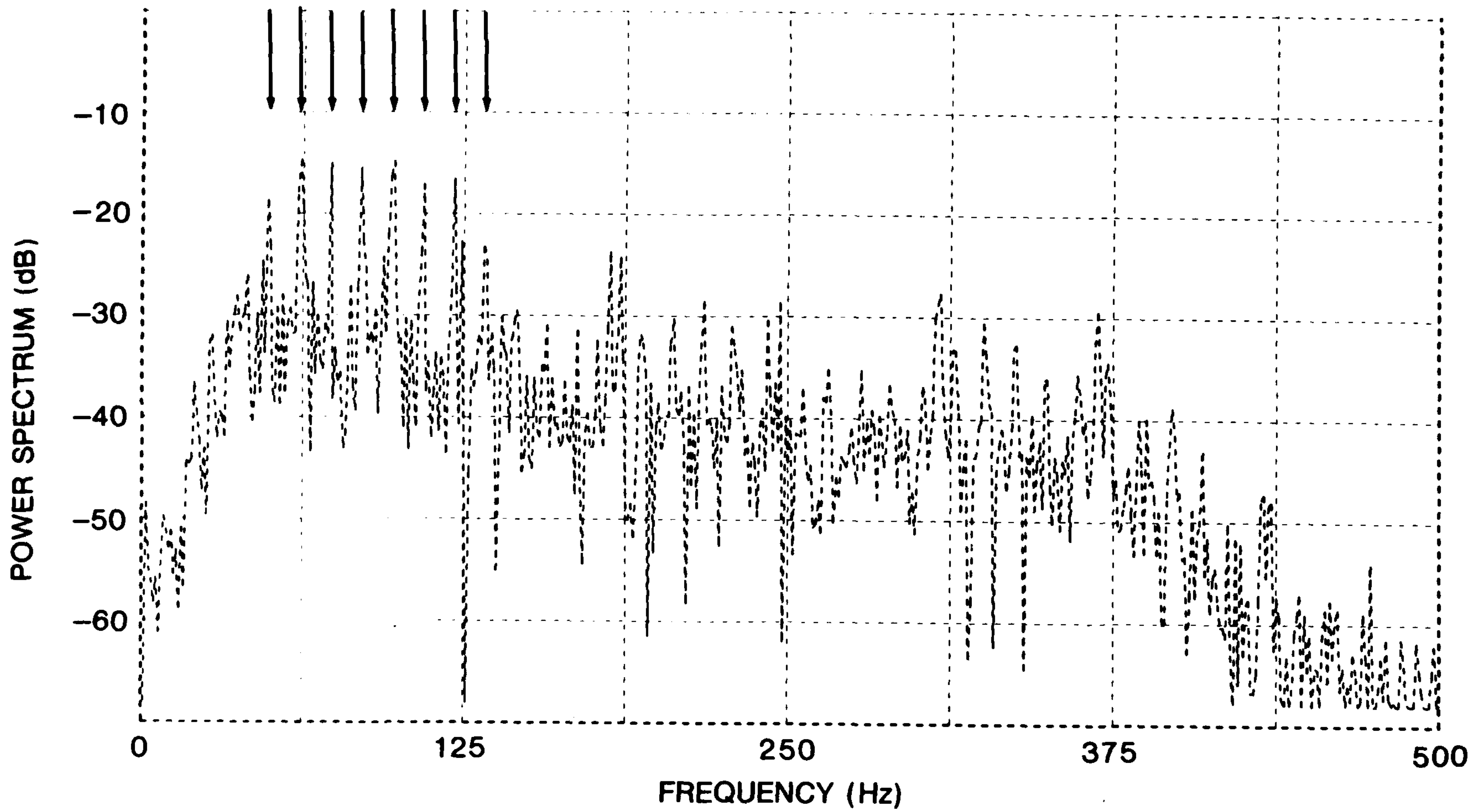

Figure 3. Power Spectrum of Helicopter-Radiated Noise. Arrows Indicate Frequency Components of Main Rotor.

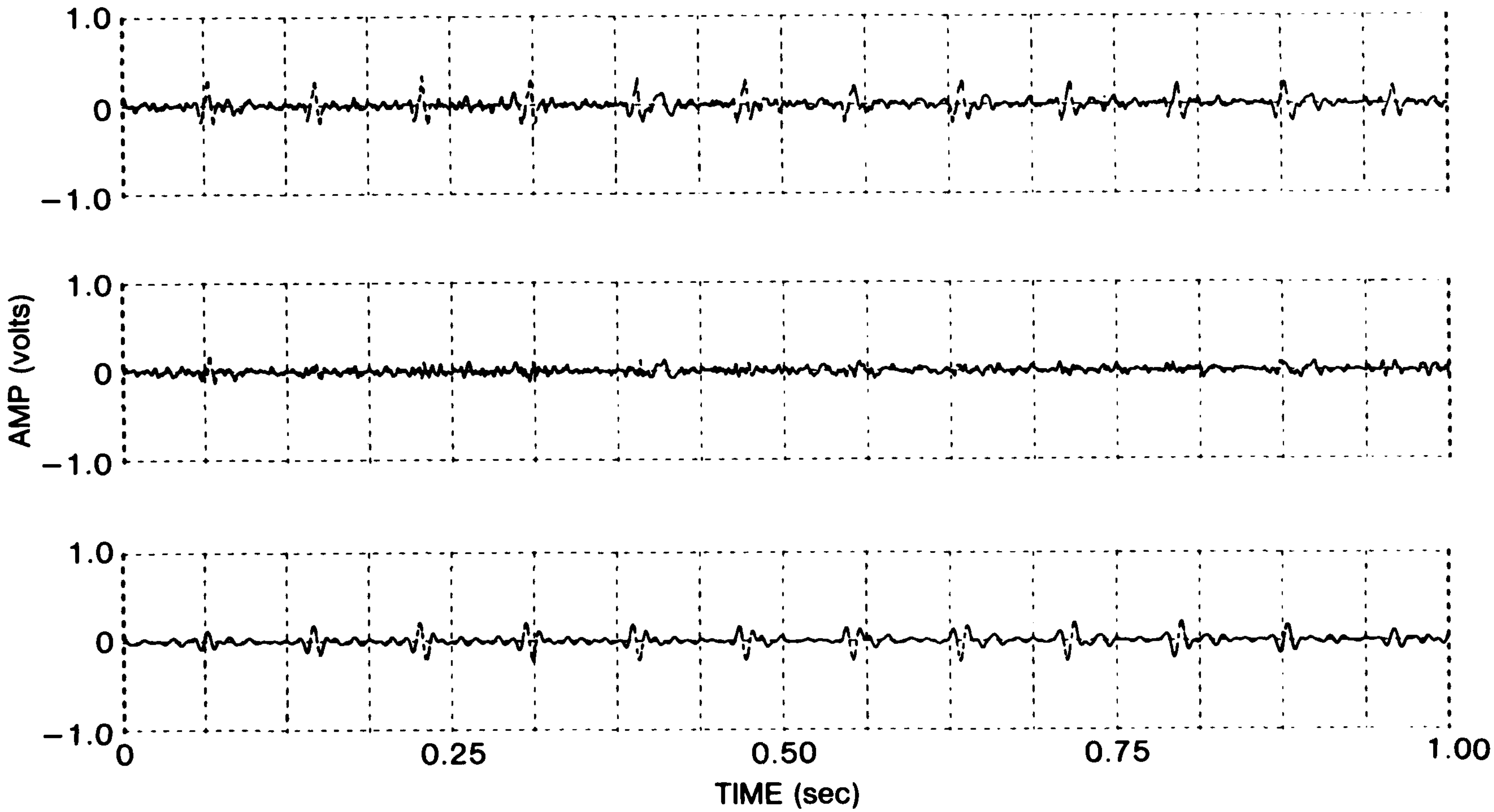

Figure 4. Time Domain data of Helicopter-Radiated Noise: Top, Original System Data; Middle; Resultant Data after Frequency Components are Extracted; Bottom, Extracted Data

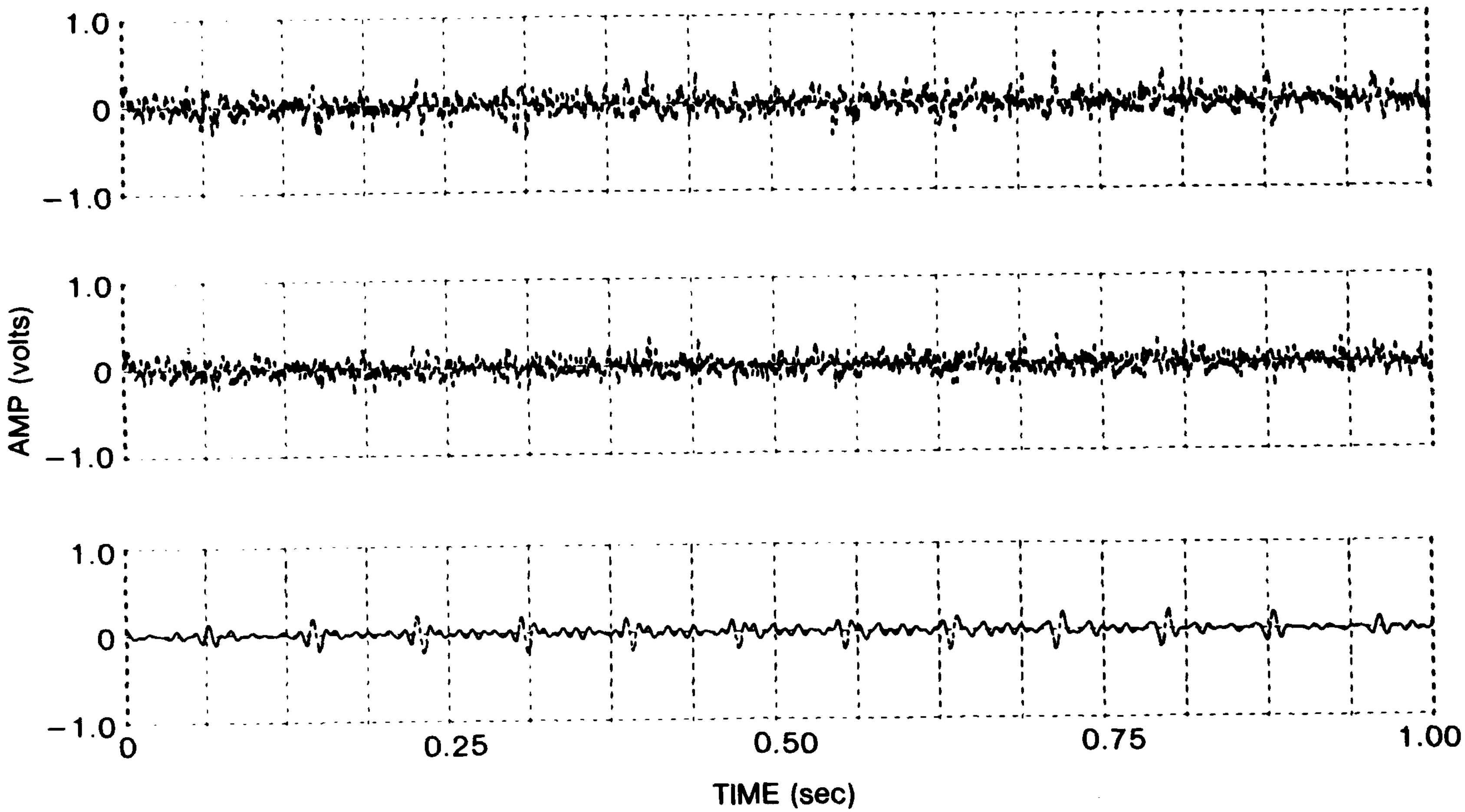

Figure 5. Time Domain Data of Helicopter-Radiated Noise in Noisy Environment: Top, Original System Data with Additive Noise at -7dB Signal-to-Noise Level; Middle, Resultant Data after Frequency Components are Extracted; Bottom, Extracted Data.

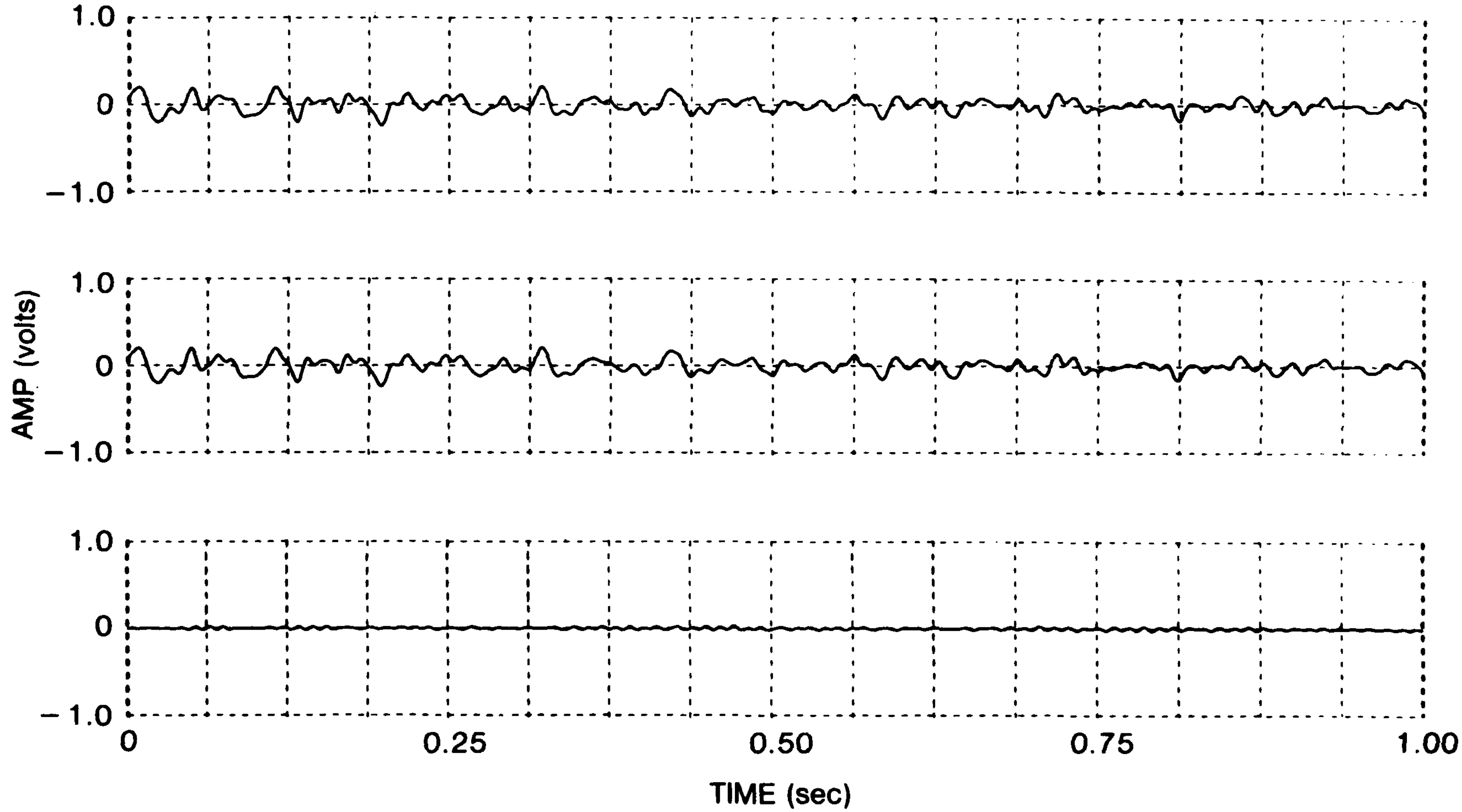

Figure 6. Sensitivity to Random Gaussian Noise: Top, Original Noise Data; Middle, Resultant Data after the Same Eight Frequency Compenents are Extracted; Bottom, Extracted Data.

MEASUREMENT AND EXTRACTION OF RECURRING TRANSIENTS:
AN APPLICATION TO THE HELICOPTER-RADIATED NOISE PROBLEM
Roger F. Dwyer
Surface Ship Sonar Department

DISTRIBUTION LIST

External

NAVSEASYSCOM (CDR. R. Schissler, Code 63D) (2 Copies)
NAVSEASYSCOM (Dr. D. Porter, Code 63R-11) (2 Copies)
ONR (Dr. N. Gerr, ONR-411) (3 Copies)
ONR (Dr. L. Johnson, ONR-425 AR) (1 Copy)

Internal

01	
02111	(A. Lotring) (2 Copies)
021311	(Library) (6 Copies)
021312	(Newport Library) (4 Copies)
03	
0302	
10	
101	(E. Hug, A. Vanwoerkom)
32	
321	
3211	
3211	(J. Fay, G. Swope, N. Owsley)
3212	
3213	
3213	(W. Struzinski)
322	
3292	
33	
331	
33A	
33A	(R. Thompkins, D. Ashworth)
33B	
33C	
3312	
3314	
3314	(E. Retherford, K. Scarbrough, I. Cohen, I. Kirsteins, D. Sheldon, A. Nuttall, E. Eby)
3314	(R. Dwyer) (20 Copies)
3315	
3315	(W. Chang, R. Paul, R. Trembly)
332	
333	

TM No. 861043

3331	(P. Koenings)
3334	
3334	(D. Klingbeil)
3335	
35	
352	
35201	
36	
363	
37	

END
FILMED

6-86

DTIC